High pressure reactivity of solid benzene probed by infrared spectroscopy

ARTICLE *in* THE JOURNAL OF CHEMICAL PHYSICS · FEBRUARY 2002

Impact Factor: 2.95 · DOI: 10.1063/1.1435570

High pressure reactivity of solid benzene probed by infrared spectroscopy

Lucia Ciabini
Dipartimento di Chimica dell'Università di Firenze, Via G. Capponi 9, I-50121 Firenze, Italy

Mario Santoro
LENS, European Laboratory for Non-linear Spectroscopy and INFM, Largo E. Fermi 2, I-50125 Firenze, Italy

Roberto Bini[a] and Vincenzo Schettino
Dipartimento di Chimica dell'Università di Firenze, Via G. Capponi 9, I-50121 Firenze, Italy and LENS, European Laboratory for Non-linear Spectroscopy and INFM, Largo E. Fermi 2, I-50125 Firenze, Italy

(Received 30 July 2001; accepted 20 November 2001)

The chemical transformation of benzene under pressure is investigated, at room temperature and at 100 K, by means of infrared spectroscopy. Pressurization-decompression cycles in the 0–50 GPa pressure range have been performed to achieve the complete transformation of the monomer. The yellow-brownish recovered sample has been identified as an amorphous hydrogenated carbon (*a*-C:H). A correlation has been established between the pressure behavior of the frequencies of both Raman and infrared internal modes, and the corresponding vibrational energies in the S_1 excited state ($^1B_{2u}$). From this comparison we conclude that pressure induces a mixing between the ground and the S_1 electronic states. The increased ring flexibility enhances the interactions among nearest-neighbor molecules inducing the formation of a network of interconnected benzene units where the aromatic character is lost. The bond breaking mainly occurs during the decompression cycle favored by the density decrease. Radical species form in this stage and rapidly propagate to give the denser *a*-C:H final product. © *2002 American Institute of Physics.*
[DOI: 10.1063/1.1435570]

I. INTRODUCTION

The application of a suitable external pressure to a molecular crystal induces a steep increase in the intermolecular interactions which become comparable to the intramolecular ones. In this framework, the molecule bond scheme can be completely altered by the delocalization of the valence electrons and new chemical species can form. This transformation can be either reversible, as in the case of CO_2[1] and O_2,[2] or irreversible, as observed for different hydrocarbons,[3–6] CO,[7] cyanogen,[8] and N_2.[9] The most important aspect of this high-pressure chemistry is that the reaction environment results greatly simplified since no catalyst is required and solvents are not present. Furthermore, since the transformation takes place in the crystal, the molecular arrangement in the lattice represents a fundamental information for the understanding of the reaction path. The static application of pressure allows also to control other important parameters such as temperature and photochemical contributions.[5]

Among the systems investigated so far, unsaturated hydrocarbons represent a major area of interest for the reactivity of the π bonds. The opening of double and triple bonds originates radical species thus triggering chain reactions. It has been demonstrated, in the case of acetylene[5] and butadiene,[10] that when specific requirements are satisfied, the pressure induced reaction can be highly ordered, even in a diamond anvil cell (DAC), and polymeric species with long-range order can be produced. More frequently a poor crystal quality, photochemical effects and strong nonhydrostatic pressure gradients determine a disordered growth. In these conditions highly branched materials (with only short-range order) are obtained. When pressure is further increased, completely amorphous products can be recovered. From this point of view the aromatic systems are of particular interest. The stability of the aromatic ring requires more drastic conditions for the reaction while the high molecular symmetry and the high electronic delocalization do not allow for the identification of preferential reaction paths. Benzene is the most suitable candidate for this kind of studies and its transformation under pressure is one of the most extensively studied.[6,11–17]

The most recent phase diagram of benzene, drawn on the basis of different spectroscopic investigations, reports five different crystal phases.[17] An additional crystal phase was detected around 22 GPa in a room temperature x-ray experiment.[13] The existence of this last phase has been confirmed, even though at lower pressure ($\simeq$17 GPa), by our recent infrared study.[18] As the pressure and temperature are raised crystalline benzene undergoes irreversible chemical reactions possibly implying the aromatic ring opening. Once benzene is heated above 870 K at 4 GPa, a black graphitic material is recovered.[11,17] The temperature of the transformation decreases very rapidly at higher pressure and materials having different colors are obtained depending on pressure and temperature values at which the chemical reaction occurs.[17] Between 6 and 11 GPa a friable and colorless com-

[a]Electronic mail: bini@chim.unifi.it

pound forms above 670 K, while a yellow-orange product is recovered when the reaction is induced in the P-T region above the limits at 670 K; 11 GPa, and 300 K; 24 GPa. The room temperature transformation was observed for the first time in an infrared absorption experiment.[6] The formation around 21 GPa of a broad band in the saturated C–H stretching region was the first signal of the onset of the reaction, but the C–H stretching bands relative to the benzene molecule were still the main peaks up to the highest pressure of the experiment (30 GPa). An indication of the occurrence of the reaction was detected in our previous infrared analysis at 23 GPa.[18] Nevertheless, all the benzene bands, including the lattice ones, were observed up to 25 GPa.

In the present work we extend our study up to 50.5 GPa using a static pressurization by means of a diamond anvil cell (DAC). The complete pressurization-decompression cycle allowed the complete transformation of benzene to an amorphous hydrogenated carbon (a-C:H) whose composition is still $(CH)_n$. The recovered compound shows some different characteristics from the analogous materials produced by chemical vapor deposition (CVD) or radio frequency sputtering (RFS). The analysis of the frequency evolution of the molecular modes provides information about the distortion of the benzene molecule at high pressure and, consequently, on the possible mechanism of the aromatic ring opening.

II. EXPERIMENT

High-pressure infrared spectra of solid benzene were measured using a membrane diamond anvil cell (MDAC) equipped with IIa diamonds. The cell was loaded by filling the gasket hole with a drop of liquid benzene from Merck (purity$\geqslant$99.9). The cell was closed maintaining the sample in the liquid phase in order to cross very slowly the melting point. This procedure ensured the production of high quality crystals in the orthorhombic phase I. The sample dimensions were typically 40–50 μm thick and 150 μm in diameter. Rhenium gaskets were employed to retain the sample at high pressures. A ruby chip was inserted in the sample to measure the local sample pressure by the R_1 ruby fluorescence band shift according to the equation $P(\mathrm{GPa}) = 248.4[(\lambda/\lambda_0)^{7.665} - 1]$.[19]

The complete apparatus to perform infrared experiments under pressure, including the optical beam condenser, has been extensively described in previous reports.[2,20] A Fourier transform infrared (FTIR) spectrometer (Bruker IFS-120 HR) was used to measure the infrared spectra. The instrument was equipped with a KBr beam-splitter and semiconductive detectors (MCT, InSb). The instrumental resolution was better than 1 cm^{-1}.

The recovered product was analyzed by Raman spectroscopy using the 514.5 and the 647.1 nm emission lines of an Ar and a Kr ion lasers, respectively. A double monochromator (U-1000, Jobyn Yvon) equipped with a CCD detector was employed to filter and detect the Raman signal. The x-ray diffraction pattern was also measured by using a Mo source, at 13 mA and 55 kV, whose emission was filtered by Zr and then focused to a 100 μm spot on the sample. An imaging plate was used to record the diffraction profile. Absorption spectra were recorded between 8000 and 40 000 cm^{-1} by using a Cary 5 spectrometer (Varian) and the FTIR spectrometer, equipped with a white lamp, a quartz beamsplitter and a InSb detector. Finally, an EPR analysis of the recovered material was performed by using a fixed microwave frequency at 9.81 GHz and a magnetic field tuned between 500 and 5500 Gauss ($14 \leqslant g \leqslant 1.27$). Sensitivity was better than 100 ppm.

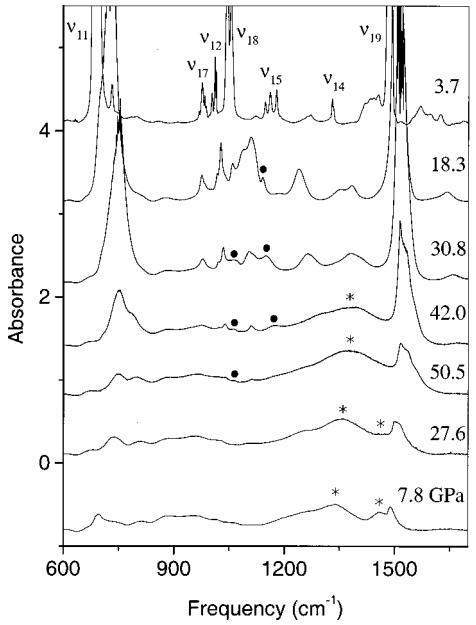

FIG. 1. Infrared absorption spectra collected along a compression–decompression cycle at room temperature. The new bands which appear at high pressure are indicated by full dots (intermediate species) or asterisks (product species).

III. RESULTS

In Figs. 1 and 2 we report some spectra collected at room temperature in the mid infrared spectral range along a typical pressurization-decompression cycle. A similar behavior has been observed at 100 K. The spectral evolution below 25 GPa has been extensively described in a previous work.[18] Above 25 GPa, an irreversible weakening and broadening of the sharp benzene bands is observed, while new broad bands, assigned to the reaction product appear in the spectrum. The most intense infrared (IR) peaks of the benzene crystal, corresponding to the ν_{11}, ν_{18}, ν_{19} and ν_{13} (or ν_{20}) modes, are still detectable up to the maximum pressure of 50.5 GPa. In particular, the absorption bands of the ν_{11} ($\sim$750 cm^{-1}) and ν_{19} ($\sim$1520 cm^{-1}) modes are saturated up to 40 GPa. Other peaks, relative to some components of the ν_{12} and ν_{17} molecular modes, are observable up to 50 GPa but with a very low intensity. When pressure is released, the intensity of all the benzene bands decreases indicating that the transformation becomes complete during this stage. Two of the new bands which appear during the compression step (indicated by full dots in Fig. 1) are detectable only in a limited pressure range. The first peak is observed above 12 GPa at 1137 cm^{-1}. Its intensity rapidly increases up to 30 GPa but a progressive weakening follows a further compression and the

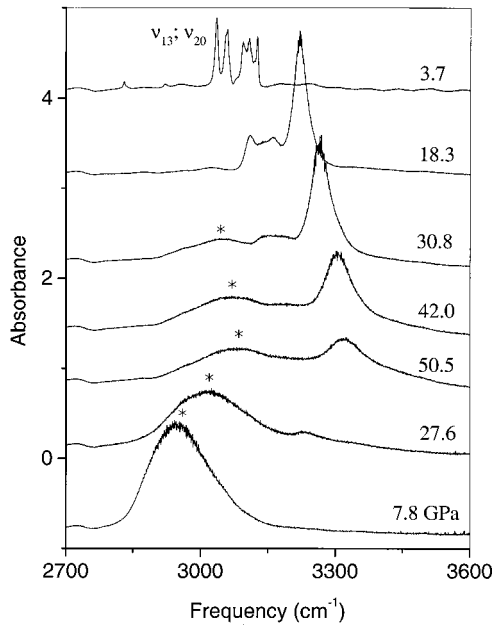

FIG. 2. Infrared absorption spectra collected along a compression–decompression cycle at room temperature in the C–H stretching spectral region of benzene. Remarkable is the disappearance of the benzene peaks with releasing pressure while the band of the product, labeled with an asterisk, strongly intensifies.

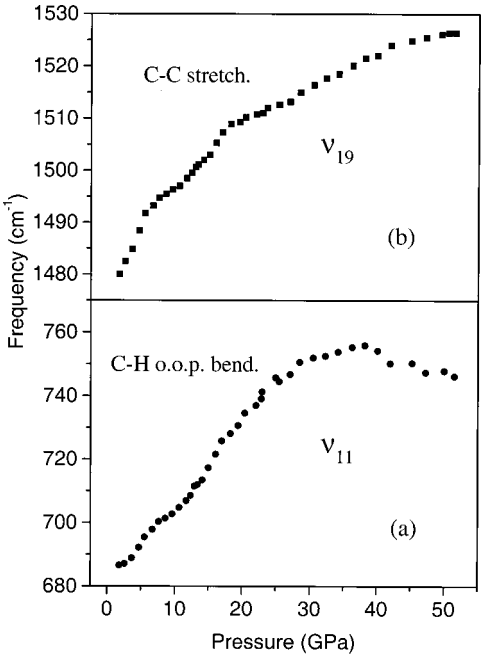

FIG. 3. Frequency evolution with pressure of the ν_{11} (a) and ν_{19} (b) modes. Below 40 GPa the frequency values of both peaks have been estimated by the saturated absorption bands.

peak disappears between 42 and 45 GPa. Another weak band is observed at 1058 cm^{-1} when pressure exceeds 25 GPa, but also this peak disappears at higher pressures. The origin of these bands is not obvious, but a reasonable explanation can be the formation of intermediate species, an aggregate of benzene molecules (probably a dimer), representing a kind of nucleation step of the chemical reaction.

The general broadness and weakness of the high pressure spectrum makes the identification of the peaks due to the reaction product not easy. The new bands appearing above 25 GPa and not due to intermediate species strongly intensify during the decompression cycle attesting that the reaction mainly occurs during this step as it is also indicated by the disappearance of the benzene bands. The most prominent product bands have been labeled by asterisks in Figs. 1 and 2. In Fig. 1 a broad band is detected above 20 GPa in the ν_{14} region (1375 cm^{-1} at 50.5 GPa). More informative are the changes occurring in the C–H stretching region which are shown in Fig. 2. Here, the strongest high frequency peak, assigned to a crystal component of the ν_{13} (or ν_{20}) benzene mode, remarkably weakens with decreasing pressure. In contrast, the broad band at lower frequency, assigned to C–H stretching modes involving sp^3 carbon atoms, rapidly intensifies when the pressure is released.

All the bands were fitted with pseudo-Voight line shapes in order to obtain the spectral parameters of interest (peak position and intensity). In Figs. 3–5 we report the frequency evolution with pressure of the crystal modes measured along the entire pressurization path. A noticeable result is that the frequency behavior at high pressure is quite different depending on the mode under investigation. The frequency values of the ν_{11} and ν_{19} modes (see Fig. 3) were estimated from the saturated absorption profiles. The frequency of the ν_{19} mode shows a continuous decrease of the slope with increasing pressure and it becomes almost flat above 40 GPa. The frequency of the ν_{11} mode shows a softening above 38 GPa thus revealing a weakening of the intramolecular chemical bonds. The region between 900 and 1200 cm^{-1} is simplified at high pressure since the number of observed components greatly reduces above 25 GPa. The frequency evolution of the modes which are observed in this spectral region up to 40–50 GPa are reported in Fig. 4. The high- and low-frequency components of the ν_{17} mode are detected up

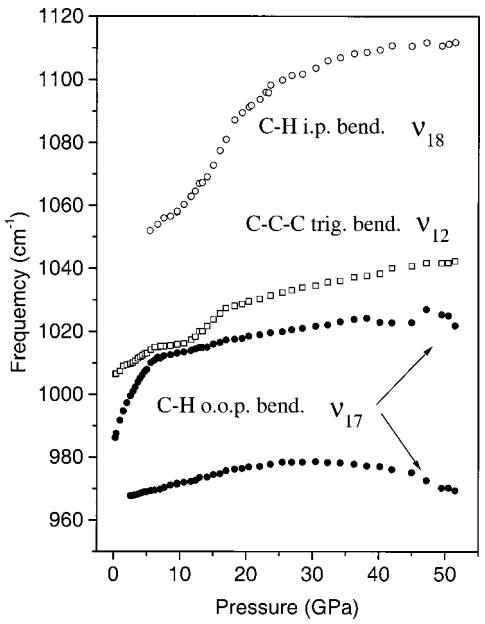

FIG. 4. Frequency evolution with pressure of the crystal components of the ν_{17}, ν_{12}, and ν_{18} internal modes.

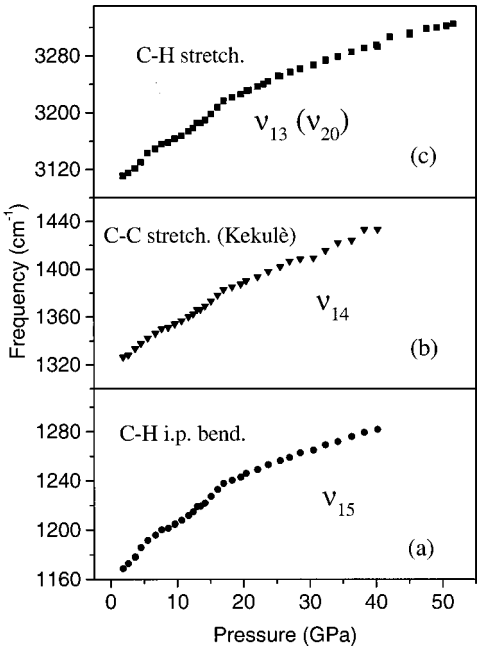

FIG. 5. Frequency evolution with pressure of the modes which exhibit a hard behavior: ν_{15} (a), ν_{14} (b), and $\nu_{13}-\nu_{20}$ (c).

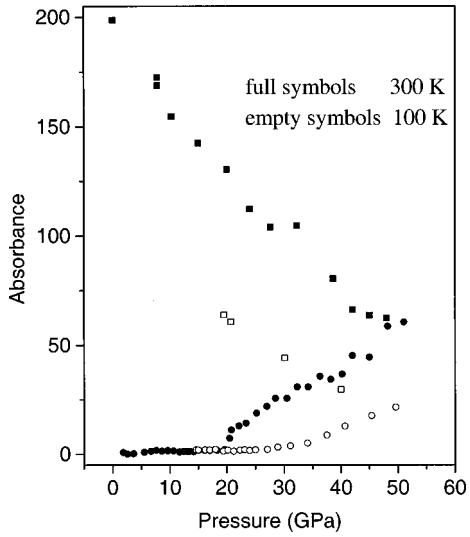

FIG. 6. Pressure evolution of the integrated absorption of the product band assigned to C–H stretching modes involving sp^3 carbon atoms (labeled by an asterisk in Fig. 2). The two sets of data have been collected at room temperature (full symbols) and at 100 K (empty symbols). The dots indicate the data collected during the compression step, while the squares correspond to the decompression cycle.

to 50.5 GPa and show different behaviors. The low-frequency component is characterized by a softening above 29 GPa thus confirming a weakening of the molecular bonds. On the contrary, the high frequency component becomes flat only above 40 GPa. In the same region only one component of the ν_{18} mode is left at high pressure showing a continuous slope decrease above 20 GPa. In Fig. 5 the evolution of the ν_{15}, ν_{14}, and ν_{13} (or ν_{20}) components are reported. The ν_{15} and ν_{14} peaks are detectable up to 40 GPa and their frequencies increase linearly above 20 GPa. The evolution with pressure of the strongest peak in the $\nu_{13}-\nu_{20}$ absorption region, visible up to the maximum pressure, also presents a similar hard behavior in spite of a very slight decrease of the slope above 40 GPa.

The most intense absorption band of the product of the reaction falls in the C–H stretching region involving saturated carbon atoms (structure labeled by asterisks in Fig. 2). The total infrared intensity in this region has been analyzed as a function of pressure during both the compression and decompression cycles. The results at room temperature and 100 K are shown in Fig. 6. It can be seen that the intensity of this feature grows during the compression stage, but by far more impressive is the rapid intensification observed when the pressure is released, indicating that most of the transformation takes place with decreasing pressure. Closer examination of the band structure in the recovered sample shows the presence of two components, as it will be discussed in the following. The behavior at room and low temperature is similar apart from the fact that at 100 K the reaction is slowed down and shifted at higher pressure (above 27 GPa).

IV. ANALYSIS OF THE RECOVERED SAMPLE

The solid material recovered at room pressure after the pressurization cycle shows an inhomogeneous yellow-brownish color when observed in transmission or in reflection. This is in partial disagreement with previous experiments where a less colored or white sample was obtained after benzene was compressed up to 30 GPa.[6,17] The difference between the final pressure of our measurement compared to previous experiments could be the reason for the discrepancy. In order to obtain information on the structural properties of the recovered sample (HP), the x-ray diffraction spectrum was measured. No Bragg peaks were detected, thus revealing the completely amorphous character of the HP sample. The amorphization is also confirmed by the irreversible disappearance, with increasing pressure, of the lattice peaks in the FIR spectral region[18] and of the whole Raman intensity.[13] No indication of hydrogen loss was noticed by visual observation (bubble formation), or from the Raman (H_2 vibron) and IR (intensity decrease of the C–H stretching modes) spectra. All these evidences suggest that the properties of this reaction product can be most likely be explained assuming that it consists of a form of amorphous hydrogenated carbons (*a*-C:H).

The infrared spectrum of the HP compound is shown in Fig. 7 (full line). An important difference with the spectrum of the recovered product reported in Ref. 6 is the lack of the C–O and C═O stretching modes. To avoid oxygen contamination care was taken to open the cell in an inert atmosphere (N_2) and to maintain the cell under vacuum during the measurement. Anyway, also the spectra recorded after the exposition to atmosphere did not show any trace of oxygen contamination. The compression up to 50 GPa allows the complete transformation of benzene and no free radicals are left after the downstroke. This has been confirmed by the electron paramagnetic resonance (EPR) analysis of the recovered material. The infrared spectrum appears to be dominated by the strong band of the C–H stretching modes. All the bands are very broad as expected for a disordered and

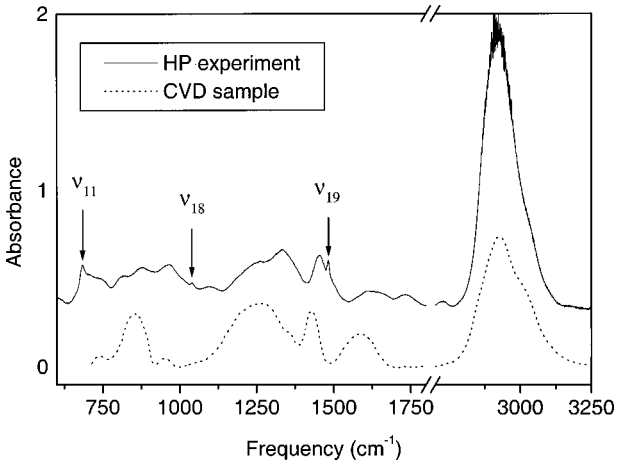

FIG. 7. The infrared spectrum of our recovered sample is reported together with that relative to an *a*-C:H obtained by benzene CVD (Refs. 25 and 26). The spectrum of the CVD sample has been rescaled in order to make it comparable to that of the HP product.

highly branched compound. Only three weak peaks (690, 1040, and 1480 cm^{-1}) are quite sharp. These bands are easily assigned to the strongest infrared modes, ν_{11}, ν_{18}, and ν_{19}, respectively, of the benzene molecule.[21] Since these peaks are detected even after the cell opening, we conclude that some benzene molecules are trapped in the final product as impurities. In Table I an assignment of all the bands observed in the spectrum of the HP sample is given on the basis of the characteristic frequencies of the benzene molecule[21] and of saturated and unsaturated long chain hydrocarbons.[22–24] In the 600–1100 cm^{-1} range interference fringes are superimposed to the spectral profile. The recovered sample thickness was measured to be 35–40 μm and, according to the interference fringes period ($\simeq$75 cm^{-1}) observed in the FTIR spectrum, a refractive index of 1.7–1.9 is estimated. This value should be compared with the value of 1.93 reported for the *a*-C:H obtained by the CVD technique.[25,26]

TABLE I. Assignment of the bands observed in the spectrum of the recovered sample. The characteristic frequencies of benzene molecule (Ref. 21) and of saturated and unsaturated long chain hydrocarbons (Refs. 22–24) have been employed.

Frequency range	Assignment
690	ν_{11} mode of benzene
700–760	CH_2 rocking[a]
	cis-CH wagging (cis-dialkyl)[b]
800–1000	CH wagging (trialkyl)[b]
	CH_2 wagging (1,1-dialkyl)[b]
	CH_2 wagging[b]
	CH_2 rock+twist[a]
	trans CH wagging[b]
1040	ν_{18} mode of benzene
1070–1120	C–C stretching[a]
1160–1300	CH_2 twisting[a]
	CH_2 wagging[a]
	CH rocking[b]
1300–1360	trans CH sym. rocking[b]
1440–1470	CH_2 bending[a]
1480	ν_{19} mode of benzene
1580–1680	C=C stretching[b]

[a]From Refs. 22 and 23.
[b]From Ref. 24.

In Fig. 7 the IR spectrum of an *a*-C:H sample obtained by benzene CVD is also reported (dotted line).[25,26] The absorbance of the CVD sample has been rescaled for an easier comparison with the HP product. The comparison between the two spectra is difficult below 1100 cm^{-1} due to the presence of the interference fringes in the HP sample. Much easier is the comparison above 1000 cm^{-1}. The three broad bands of the CVD sample present a full correspondence with similar peaks in the spectrum of the HP sample even though in the latter the bands are blue-shifted by 50–100 cm^{-1}. In the C–H stretching region the bands of the two samples have the same frequency position, but a stronger intensity is observed in the HP product, suggesting a higher hydrogen content. The blue shift observed in the HP sample spectrum can be explained assuming that in the sample there is a certain amount of olefinic chains. It is known that the vibrational frequencies in such systems move to lower energy as the chain length increases.[22,23] For a given Csp^2/Csp^3 ratio longer olefinic chains imply a lower H/C ratio, and the excess carbon atoms can actually originate graphitic clusters that are detected in CVD samples by Raman[27,28] and UV-VIS absorption measurements.[25,26] Alternatively, the blue shift could be ascribed to a residual internal strain in the recovered HP sample. As a matter of fact, the elevated stiffness of the *a*-C:H (greater than that of sapphire[26]) is related to the high degree of internal strains which depends on the preparation procedure. After the cell is opened measurement of the fluorescence of a ruby fully incorporated in the sample gives a residual pressure of $\sim$1.3 GPa. This, together with the significant distortion of the ruby fluorescence doublet, is a clear evidence of a strong nonisotropic residual strain in the sample.

The Raman spectrum of the HP sample does not show any band when either the 514.5 nm (Ar^+) or the 647.1 nm (Kr^+) excitation lines are employed. The same observation was reported for the recovered samples from lower pressure experiments.[6,17] On the other hand, the spectra of the *a*-C:H, produced by CVD techniques, are characterized by two broad bands at about 1330 (D) and 1580 (G) cm^{-1} assigned to graphite.[27–29] The lack of these bands in our spectrum can be due to a larger hydrogen concentration than in the CVD sample for which a value of 35% has been reported.[27] A larger hydrogen content reduces the possibility of formation of graphite clusters or quaternary carbons. As already mentioned, we have no evidence of hydrogen loss thus suggesting a composition having a H/C ratio close to one. Another indication of the high hydrogen content is given by the measurement of the optical gap. In *a*-C:H samples the energy of the gap ranges from 0.5 to 2.5 eV, depending on the decreasing graphitic character, i.e., the increasing hydrogen content. Dischler *et al.*[25,26] measured the optical gap of *a*-C:H samples having an H/C ratio ranging between 0.5 and 0.65 and observed a linear increase of the gap energy from 0.8 to 1.8 eV. These samples represent a good test for a direct comparison with the HP material due to the strong similarities of the infrared spectra (see Fig. 7). Our HP sample is transparent up to 2.0 eV, while above this energy the absorbance

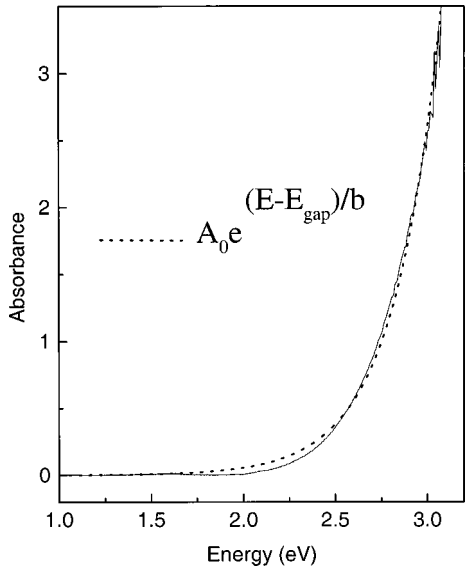

FIG. 8. Absorption edge of the recovered HP sample. The dotted line is the best fit of the experimental profile according to the exponential law reported in the figure. The parameters employed in the fit are: $A_0=0.38$; $E_{gap}=2.5$ eV; $b=0.26$ eV.

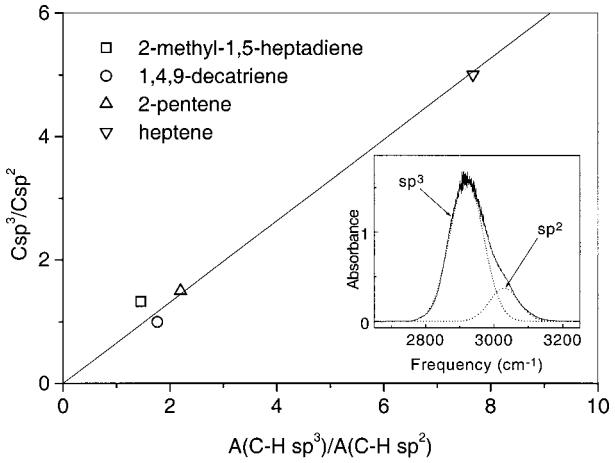

FIG. 9. Dependence of the Csp^3/Csp^2 quantity on the ratio of the integrated area of C–H stretching modes involving sp^3 and sp^2 carbon atoms. The data points have been obtained by the infrared spectra of selected molecules having unconjugated double bonds. A linear fit of this evolution is also reported. In the inset we report an example of the deconvolution of the broad structure in two peaks, centered at 2920 and 3030 cm^{-1}, and assigned to the C–H stretching modes involving sp^3 and sp^2 carbon atoms, respectively.

increases exponentially (see Fig. 8). An exponential fit of the absorption profile locates the gap at 2.5 eV thus suggesting an H/C ratio close to one. Only calculations are available for samples where graphite clusters are completely absent; in this case the band gap is calculated at 3 eV.[30]

Beside the hydrogen content, another important information on the structure of the HP sample can be given by the relative amount of sp^3 and sp^2 carbon sites. The mechanical properties of the material are strictly connected with the relative abundance of these two sites. Their ratio can be directly estimated by means of NMR (nuclear magnetic resonance)[31] or EELS (electron energy loss spectroscopy).[32] Both techniques are not easily applied to our HP samples and, therefore, we tried to estimate this ratio from the available infrared data. For this purpose the ratio of the integrated area of the C–H stretching bands relative to sp^3 and sp^2 carbon atoms was already employed in previous studies.[25,26] As already noted above, the unresolved structure between 2800 and 3100 cm^{-1} can be deconvoluted in two broad bands centered at 2920 and 3030 cm^{-1} as shown in the inset of Fig. 9. The low- and high-frequency peaks are assigned to C–H stretching modes involving, respectively, sp^3 and sp^2 carbon atoms. In Refs. 25 and 26 the ratio between the integrated intensity of the two peaks was directly correlated to the Csp^3/Csp^2 sites ratio. This procedure neglects the different transition strength of the stretching modes involving saturated and unsaturated carbon atoms. To partly overcome this limitation, at least at a semiquantitative level, we constructed a kind of reference diagram (see Fig. 9). We built this diagram by considering, in a series of molecules of increasing complexity, the ratio of the intensities of saturated to unsaturated C–H stretching modes as a function of the relative abundance of sp^3 and sp^2 carbon atoms. Molecules with no sp^3 quaternary or methylic carbons were used since no evidences of these species have been found in NMR studies of *a*-C:H carbons.[31] It is seen from Fig. 9 that the reference data can fit on a linear relation. Using this diagram it is found that the observed infrared intensity ratios of 4.9 and 2.3 for the HP and CVD samples, respectively, lead to Csp^3/Csp^2 ratios of 3.2 and 1.5, i.e., to 76% and 60% abundance of sp^3 carbon atoms. This agrees with a higher hydrogen content in the HP sample.

V. THE REACTION MECHANISM

When the results of calculation[14] are compared with Raman experiments[13] a good agreement is found for the phonon and the symmetric C–C and C–H stretching modes for pressures up to ~20 GPa. In contrast, for the doubly degenerate C–C–C and a C–H bending modes (ν_6 and ν_{10}, respectively) the frequency increase with pressure is lower than calculated. Thiery *et al.*[14] interpreted this behavior as due to a distortion of the benzene molecule at high pressure as a result of a mixing between the ground and the lowest excited electronic levels through a vibronic coupling. According to these authors the behavior of the infrared active modes could be a crucial test to ascertain whether the symmetry and nature of the internal motions are important in triggering the high pressure reaction.

In the infrared spectrum it has been reported that up to 20 GPa all the modes exhibit appreciable changes of the frequency, linewidth and integrated absorption intensity along the different crystalline phase transitions.[18] The situation is quite different at higher pressures. In fact, a remarkable softening with increasing pressure is observed for the lowest frequency component of the ν_{17} and ν_{11} modes, as it can be seen from Figs. 3 and 4. On the other side, the remaining component of ν_{18} becomes flat at pressure higher than 40 GPa, and a very similar behavior is also observed for the high-frequency component of ν_{17}. In contrast, all the other modes still detectable at high pressure show a continu-

TABLE II. Vibrational frequencies (cm^{-1}) in the $^1A_{1g}$, $^1B_{2u}$, and $^3B_{1u}$ states of benzene Refs. 34 and 35. Percentage variations $\Delta\nu/\nu$ between the frequencies in the ground and in the $^1B_{2u}$ (S_1) and $^3B_{1u}$ (T_1) excited states are also reported.

Mode	Symm.	$^1A_{1g}$	$^1B_{2u}$	$^3B_{1u}$	$\Delta\nu/\nu$ % ($^1B_{2u}$)	$\Delta\nu/\nu$ % ($^3B_{1u}$)
ν_1	a_{1g}	993	923	925	−7.0	−7.0
ν_2	a_{1g}	3074	3093		0.6	
ν_3	a_{2g}	1350	1327		−2.0	
ν_4	b_{2g}	707	365		−48.0	
ν_5	b_{2g}	990	745		−25.0	
ν_6	e_{2g}	608	521	628	−14.0	3.0
ν_7	e_{2g}	3057	3077		0.6	
ν_8	e_{2g}	1600	1516	245	−5.0	−85.0
ν_9	e_{2g}	1178	1148	1188	−2.0	0.8
ν_{10}	e_{1g}	847	581		−31.0	
ν_{11}	a_{2u}	674	515		−23.0	
ν_{12}	b_{1u}	1010	936		−7.0	
ν_{13}	b_{1u}	3057	3159		3.0	
ν_{14}	b_{2u}	1310	1570		19.0	
ν_{15}	b_{2u}	1149	1150		0.1	
ν_{16}	e_{2u}	399	238	244	−40.0	−39.0
ν_{17}	e_{2u}	967	717		−26.0	
ν_{18}	e_{1u}	1038	920		−11.0	
ν_{19}	e_{1u}	1484	1405		−5.0	
ν_{20}	e_{1u}	3065	3084		0.6	

ous hardening even though with different slopes from mode to mode. This behavior can be explained as arising from a benzene ring distortion at high pressure, while the differences exhibited by modes of similar type suggest that the distortion should correspond to a precise geometry. This behavior is reminiscent of the shear deformation effect discussed by Gilman[33] in the compression induced insulator (or semiconductor) to metal transition. A clue to understanding this behavior was gained from the comparison of the vibrational frequencies of benzene in the ground $^1A_{1g}(S_0)$ and first excited singlet $^1B_{2u}(S_1)$ and triplet $^3B_{1u}(T_1)$ states.[34,35] As it can be seen from Table II it turns out that all the u internal modes showing a softening or a flat evolution at high pressure (ν_{11}, ν_{17}, and ν_{18}) and, likewise, the g modes which show a softer behavior compared to calculation (ν_6 and ν_{10}) correspond to modes whose frequency shows a remarkable (larger than 10%) lowering in the S_1 excited state. On the other hand, the modes showing a continuous hardening with increasing pressure (ν_{13}, ν_{14}, ν_{15}, and ν_{20}) have a higher frequency in the S_1 state. A strong lowering of the frequency in the S_1 state is also found for the ν_4, ν_5, and ν_{16} modes, but these modes are all too weak to be observed in high-pressure experiments. In Table II the available vibrational frequencies for the $T_1(^3B_{1u})$ excited state are also reported.[34] In particular the large frequency lowering of the ν_8 mode and the small frequency increase of the ν_6 mode do not match with the data reported in Ref. 14. In conclusion, the correlation found with the change of the vibrational frequencies in the S_1 state suggests that changes in geometry induced by high pressure should be similar to those occurring in the first excited state. On the other hand, an energy lowering of the electronic excited states at high pressure is a quite general effect. The lowering of the energy gap between ground and excited states enhances a progressive mixing of these states, a process that can be particularly significant when the changes in the equilibrium geometry are large. In this case the transition can be thermally activated even though the optical transitions are still rather high in energy.[36] A thermal activation of the electronic transition would also explain the occurrence of the reaction at higher pressure in the low temperature experiment (see Fig. 6), even though the decreased amplitude of the lattice motions with lowering temperature is expected to determine the same effect[37] as also recently demonstrated by a study on the pressure induced reaction of solid acetylene.[5]

At this stage one can envisage the following reaction path for the high-pressure transformation of benzene. At high pressure a progressive mixing of the ground and first excited singlet state occurs. According to the molecular arrangement in the crystal at pressure close to the onset of the reaction,[16] an effective overlap of the π clouds of neighboring molecules takes place. The high ring flexibility favors the interaction with the nearest neighbor molecules and the electronic charge density transfers toward the intermolecular region. Therefore, at high pressure the sample behaves as a network of strongly interacting distorted rings. This explains the persistence of the benzene vibrational modes even at the highest pressure of the present experiment. In these conditions differences between intra and intermolecular interactions are extremely reduced and new bonds between carbon atoms of different molecules start to be formed. However, the high density of the pressurized sample, i.e., the small available molecular volume, prevents an extended reconstruction of the chemical bonds. When the pressure is released, and the molecular volume available increases, the intramolecular bonds can break down and the ring opening produces radical species which rapidly propagate the formation of an extended network of saturated carbon–carbon bonds.

VI. CONCLUSIONS

The chemical transformation of benzene under pressure has been fully investigated by means of infrared spectroscopy. A correspondence between the pressure evolution of the internal modes frequency and the molecular vibrational levels in the S_1 state suggests that the chemical transformation is favored by the pressure induced mixing of the S_0 and S_1 electronic states. This kind of coupling determines an increasing molecular instability with pressure which drives the strengthening of the interaction among nearest neighbor molecules. The reaction occurs mainly releasing pressure through the opening of the benzene rings and the rapid propagation by radical species. The recovered sample is an amorphous hydrogenated carbon with peculiar characteristics when compared to those obtained by other common preparation techniques (CVD). The absence of carbon clusters and the high hydrogen content, which is preserved during the reaction in the DAC, are remarkable characteristics of the a:C–H prepared with the high-pressure reaction.

ACKNOWLEDGMENTS

The authors gratefully acknowledge the help of F. Gorelli and J. Haines for the x-ray diffraction experiment and

S. Ristori for the EPR measurements on the recovered sample. This work has been supported by the European Union under Contract HPRI-CT1999-00111 and by the Italian Ministero dell'Universitá e della Ricerca Scientifica e Tecnologica (MURST).

[1] C. S. Yoo, H. Cynn, F. Gygi, G. Galli, V. Iota, M. Nicol, S. Carlson, D. Häusermann, and C. Mailhiot, Phys. Rev. Lett. **83**, 5527 (1999).
[2] F. Gorelli, M. Santoro, L. Ulivi, and R. Bini, Phys. Rev. Lett. **83**, 4093 (1999).
[3] K. Aoki, S. Usuba, M. Yoshida, Y. Kakudate, K. Tanaka, and S. Fujiwara, J. Chem. Phys. **89**, 529 (1988).
[4] M. Sakashita, H. Yamawaki, and K. Aoki, J. Phys. Chem. **100**, 9943 (1996).
[5] M. Ceppatelli, M. Santoro, R. Bini, and V. Schettino, J. Chem. Phys. **113**, 5991 (2000).
[6] Ph. Pruzan, J. C. Chervin, M. M. Thiery, J. P. Itie, and J. M. Besson, J. Chem. Phys. **92**, 6910 (1990).
[7] A. I. Katz, D. Schiferl, and R. L. Mills, J. Phys. Chem. **88**, 3176 (1984).
[8] C. S. Yoo and M. Nicol, J. Phys. Chem. **90**, 6732 (1986).
[9] A. F. Goncharov, E. Gregoryanz, H. K. Mao, Z. Liu, and R. J. Hemley, Phys. Rev. Lett. **85**, 1262 (2000).
[10] M. Citroni, M. Ceppatelli, R. Bini, and V. Schettino, Science (unpublished).
[11] S. Block, C. E. Weir, and G. J. Piermarini, Science **169**, 586 (1970).
[12] M. Nicol, M. L. Johnson, and N. C. Holmes, Physica B **139–140**, 582 (1986).
[13] M. M. Thiery and J. M. Leger, J. Chem. Phys. **89**, 4255 (1988).
[14] M. M. Thiery, J. M. Besson, and J. L. Bribes, J. Chem. Phys. **96**, 2633 (1992).
[15] J. M. Besson, M. M. Thiery, and P. Pruzan, in *Molecular Systems Under High Pressure*, edited by R. Pucci and G. Piccitto (Elsevier, Amsterdam, 1991), p. 341.
[16] M. Gauthier, J. C. Chervin, and P. Pruzan, in *Frontiers of High Pressure Research*, edited by H. D. Hochheimer and R. D. Etters (Plenum, New York, 1991), p. 87.
[17] F. Cansell, D. Fabre, and J. P. Petitet, J. Chem. Phys. **99**, 7300 (1993).
[18] L. Ciabini, M. Santoro, R. Bini, and V. Schettino, J. Chem. Phys. **115**, 3742 (2001).
[19] H. K. Mao, P. M. Bell, J. V. Shaner, and D. J. Steinberg, J. Appl. Phys. **49**, 3276 (1978).
[20] R. Bini, R. Ballerini, G. Pratesi, and H. J. Jodl, Rev. Sci. Instrum. **68**, 3154 (1997).
[21] G. Varsányi, *Vibrational Spectra of Benzene Derivatives* (Academic, New York, 1969).
[22] R. G. Snyder and J. H. Schachtschneider, Spectrochim. Acta **19**, 85 (1963).
[23] J. H. Schachtschneider and R. G. Snyder, Spectrochim. Acta **19**, 117 (1963).
[24] *Infrared and Raman Characteristic Frequencies of Organic Molecules*, edited by D. Lin-Vien, N. B. Colthup, W. Fateley, and J. G. Grasselli (Academic, San Diego, 1991).
[25] B. Dischler, A. Bubenzer, and P. Koidl, Solid State Commun. **48**, 105 (1983).
[26] B. Dischler, A. Bubenzer, and P. Koidl, Appl. Phys. Lett. **42**, 636 (1983).
[27] M. Ramsteiner and J. Wagner, Appl. Phys. Lett. **51**, 1355 (1987).
[28] R. Vuppuladhadium, H. E. Jackson, and R. L. C. Wu, J. Appl. Phys. **77**, 2714 (1995).
[29] R. O. Dillon, J. A. Woollam, and V. Katkanant, Phys. Rev. B **29**, 3482 (1984).
[30] J. L. Brédas and G. B. Street, J. Phys. C **18**, L652 (1985).
[31] S. Kaplan, F. Jansen, and M. Machonkin, Appl. Phys. Lett. **47**, 750 (1985).
[32] J. Fink, T. Muller-Heinzerling, J. Pfluger, B. Scheerer, B. Dischler, P. Koidl, A. Bubenzer, and R. E. Sah, Phys. Rev. B **30**, 4713 (1984).
[33] J. J. Gilman, Philos. Mag. B **67**, 207 (1993).
[34] L. D. Ziegler and B. S. Hudson, in *Excited States* (Academic, New York, 1982), Vol. 5, p. 41.
[35] R. Berger, C. Fischer, and M. Klessinger, J. Phys. Chem. A **102**, 7157 (1998).
[36] H. G. Drickamer and C. W. Frank, *Electronic Transitions and the High Pressure Chemistry and Physics of Solids* (Chapman and Hall, London, 1973).
[37] T. Luty and C. J. Eckhardt, in *Reactivity of Molecular Solids*, edited by E. Boldyreva and V. Boldyrev (Wiley, Chicester, 1999), p. 51.